

complexes **28**, **38**, **33**, and **34**. Since the sign of $^1J(\text{P},\text{F})$ in these metal complexes can be assumed to be negative⁵² from the two-dimensional correlation experiments (cf. Figure 4b), it follows that $^2J(\text{F},\text{Fe})$ is positive. Of particular value is the combination of two-dimensional experiments, e.g. ($^1\text{H}, ^{57}\text{Fe}$) and ($^{31}\text{P}, ^{57}\text{Fe}$) for complex **1**. In this way, the relative signs of a variety of scalar couplings in quasitrigonal and -tetragonal complexes can be obtained (cf. Chart IV). To the best of our knowledge, the signs

of $J(\text{Fe},\text{X})$ couplings have not hitherto been reported.

Registry No. **1**, 84283-30-7; **2**, 110118-63-3; **3**, 110118-62-2; **4**, 51509-20-7; **5**, 115161-07-4; **6**, 97959-87-0; **7**, 115161-08-5; **8**, 115161-09-6; **9**, 115161-10-9; **10**, 115161-11-0; **11**, 115161-12-1; **12**, 78192-57-1; **13**, 78192-62-8; **14**, 110118-41-7; **15**, 94585-62-3; **16**, 110118-38-2; **17**, 115161-13-2; **18**, 51509-19-4; **19**, 110118-44-0; **20**, 110118-48-4; **21**, 115161-14-3; **22**, 110118-53-1; **23**, 110118-52-0; **24**, 97959-85-8; **25**, 115161-15-4; **26**, 115161-16-5; **27**, 115161-17-6; **28**, 115161-18-7; **29**, 115161-19-8; **30**, 115161-20-1; **31**, 115161-21-2; **32**, 115161-24-5; **33**, 115161-22-3; **34**, 115224-90-3; **35**, 115161-23-4; **36**, 110118-78-0; **37**, 110118-82-6; **38**, 94585-64-5.

(52) Staplin, D. C.; Parry, R. W. *Inorg. Chem.* **1979**, *18*, 1473.

Observation of Molecular Reorientation in Ice by Proton and Deuterium Magnetic Resonance

R. J. Wittebort,*† M. G. Usha,† D. J. Ruben,‡ D. E. Wemmer,§ and A. Pines§

Contribution from the Department of Chemistry, University of Louisville, Louisville, Kentucky 40292, Francis Bitter National Magnet Laboratory, Massachusetts Institute of Technology, Cambridge, Massachusetts 02139, and Department of Chemistry, University of California, Berkeley, Berkeley, California 94720. Received December 31, 1987

Abstract: We have directly observed molecular reorientation in polycrystalline hexagonal ice, ice I_h , by deuterium NMR and deuterium-decoupled proton NMR. The dynamics are seen as exchange broadening of powder patterns. The reorientational rates required to produce similar effects on the patterns are scaled according to the magnitudes of the anisotropic spin interactions, ~ 6 kHz for the proton-shielding anisotropy or ~ 200 kHz for the deuterium quadrupolar coupling in water. Because of the differing sizes of these two interactions, the two methods are complementary for studying reorientation over the temperature range 200–267 K. The results show that water molecules reorient with tetrahedral symmetry in ice. Line-shape simulations using the assumption of tetrahedral reorientation are in accord with the experimental spectra and give rates directly comparable to the temperature-dependent Debye correlation time, τ_D , from dielectric relaxation.

We report here the direct observation by deuterium and proton magnetic resonance of tetrahedral jump motions in normal hexagonal ice I_h . This result returns one to Pauling's 1935 observation that, in ice I_h , where each oxygen is tetrahedrally surrounded by four half-hydrogens, there is no single hydrogen-bonding configuration for the crystal.¹ Thus, the orientation of each molecule is not uniquely specified. With the attendant combinatorial consequences, Pauling accurately estimated the known² residual entropy as $Nk_B \ln(3/2)$. Improvements in Pauling's calculation³ and a neutron diffraction structure directly showing the disorder in the deuterium positions of hexagonal D_2O^4 have confirmed the correctness of the original idea. The question then arises as to whether or not ice molecules can interconvert among the different crystal configurations and, if so, at what rate and by what molecular mechanism(s). Ice has a measurable conductivity and a substantial polarizability (large ϵ_0), suggesting that different configurations could be generated by proton transfer and by molecular rotation. The rate question has been addressed by studying the effects of electric field jumps on conductivity⁵ and by measurements of dielectric relaxation.^{6,7} In the latter, the characteristic Debye correlation time, $\tau_D \sim 10^{-5}$ s at about 263 K, is related in some way to dipole moment reorientation resulting either from proton transfer or molecular rotation. Auty and Cole⁶ declined to interpret their dielectric relaxation experiments in terms of either of these possibilities but noted that the relaxation process is characterized by a single relaxation time and a large activation energy, $E_A = 13.5$ kcal/mol, or about 3 times the hydrogen-bond energy. Bjerrum⁸ addressed the matter of how water molecules

reorient in ice without violating the Bernal-Fowler rules for hydrogen bonding. He assumed that a small concentration of orientational defects, so-called D (two hydrogens between oxygens) and L defects (no hydrogens between oxygens), naturally occur. Once a defect is formed, neighboring waters are then relatively free to rotate with consequent relocation of the defect, but without creating additional H-bonding mismatches in the lattice. Eisenberg and Kauzman, in their standard monograph,⁹ assumed the dielectric relaxation to arise from reorientation and, on the basis of theoretical considerations, approximately equated the rotational correlation time with the dielectric correlation time; i.e., $\tau_c \sim \tau_D$. This connection thus suggests that a water molecule, at a temperature just below the freezing point, experiences $\sim 10^5$ reorientations/s. Gränicher et al. have argued, however, that in ice interconversion among the $(3/2)^N$ configurations does not occur by molecular rotation.⁷

The methods used here^{10,11} directly detect molecular reorientation by exchange modulation of the deuterium quadrupolar

- (1) Pauling, L. *J. Am. Chem. Soc.* **1935**, *57*, 2680.
- (2) Giaque, W. F.; Ashley, M. *Phys. Rev.* **1933**, *43*, 81.
- (3) Nagle, J. F. *J. Math. Phys. (Cambridge, Mass.)* **1966**, *7*, 1484.
- (4) Peterson, S. W.; Levy, H. A. *Acta Crystallogr.* **1957**, *10*, 70.
- (5) Eigen, M. *Angew. Chem., Int. Ed. Engl.* **1964**, *3*, 1.
- (6) Auty, R. P.; Cole, R. H. *J. Chem. Phys.* **1952**, *20*, 1309.
- (7) Gränicher, H.; Jaccard, C.; Scherrer, P.; Steinemann, A. *Discuss. Faraday Soc.* **1958**, *23*, 50.
- (8) Bjerrum, N. *Science (Washington, D.C.)* **1951**, *115*, 385.
- (9) Eisenberg, D.; Kauzman, W. *The Structure and Properties of Water*; Oxford University: Oxford, 1969.
- (10) Wemmer, D. E. Report LBL-8042; University of California, Berkeley: Berkeley, CA, 1978.
- (11) Wittebort, R. J.; Woehler, S. E.; Bradley, C. A. *J. Magn. Reson.* **1986**, *67*, 143.

*University of Louisville.

†Massachusetts Institute of Technology.

§University of California, Berkeley.

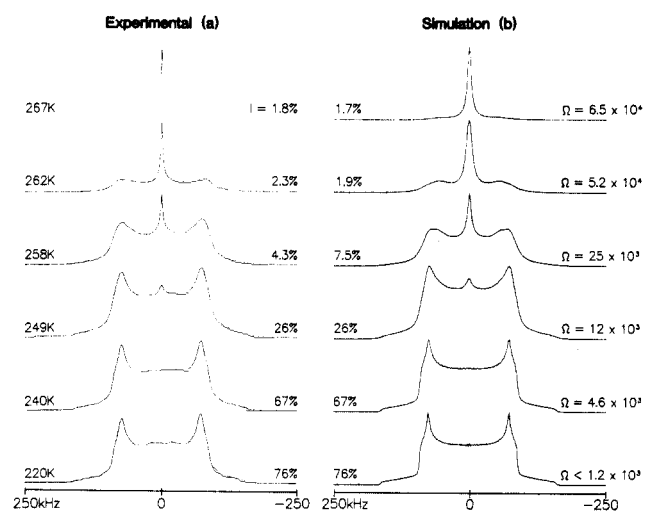


Figure 1. Experimental (a) and simulated (b) ^2H spectra of hexagonal D_2O as a function of temperature. All spectra are shown at the same vertical height and obtained with a solid-echo delay of 21 μs except at 262 K where $\tau = 25 \mu\text{s}$. I is the spectrum integral relative to the 220 K spectrum extrapolated experimentally (a) or theoretically (b) to zero echo delay ($\tau = 0$) and corrected for the Boltzman polarization. The exchange rate is $\Omega = 1/\tau_c$.

coupling or proton-shielding tensors, which have fixed orientations in the molecular frame. As discussed below, both tensors are nearly axially symmetric; thus, symmetry requirements put the unique tensor axis approximately along the O–D or O–H bonds. Consequently, these experiments report on the reorientation of this bond. Furthermore, these experiments are unaffected by the most likely type of proton transfer: that between the two neighboring oxygens to which the proton is bonded. Since the O–H...O bonding is linear, proton transfer does not reorient the tensor (shielding or quadrupolar) axis. Proton transfer between nonneighboring oxygens, however, will be included in the overall rates determined here. The results presented from ^1H and ^2H NMR are complementary in that, as in any NMR exchange study, the exchange effects are scaled according to the size of the spectral splitting, i.e., the quadrupolar coupling constant of ~ 200 kHz for the deuterium spectra and the proton-shielding tensor of ~ 6 -kHz breadth for the proton spectra.

Experimental Section

Spectra were obtained on 4.5 T (^1H) and 5.9 T (^2H) spectrometers previously described.^{10,11} The ^1H spectra were deuterium decoupled¹⁵ and recorded with a 60-s recycle delay. ^2H spectra were recorded with a solid-echo pulse sequence using 90° pulses of 2.7- μs duration. Recycle delays, varying from 10 s at 267 K to 360 s at 220 K, were chosen to ensure that spectra were obtained at full unsaturated intensity.

Samples in this work were from commercially available spectroscopic grade D_2O obtained from Bio-Rad Laboratories (^1H spectra) and MSD Isotopes or Cambridge Isotope Laboratories (^2H spectra). One sample used in the ^2H studies was vacuum distilled and vacuum sealed and gave results equivalent to those from other samples. The sample used in the ^1H spectroscopy was doped to 0.5% with distilled water and sealed under vacuum whereas the samples for ^2H spectroscopy were sealed in the atmosphere in 0.25-in.-o.d. Delrin tubes.

Results and Discussion

Shown in Figure 1a are a series of ^2H NMR spectra obtained from a polycrystalline sample of D_2O over the temperature range 220–267 K with the solid-echo pulse sequence. The spectrum at the lowest temperature, 220 K, shows the expected shape: a large coupling constant, $e^2qQ/h = 216$ kHz, and noticeable asymmetry, $\eta = 0.1$. These values are in excellent agreement with those reported previously by single-crystal measurements¹² but substantially larger than the value of $e^2qQ/h = 195$ kHz determined from a polycrystalline sample.¹³ At 286 K, not shown, these

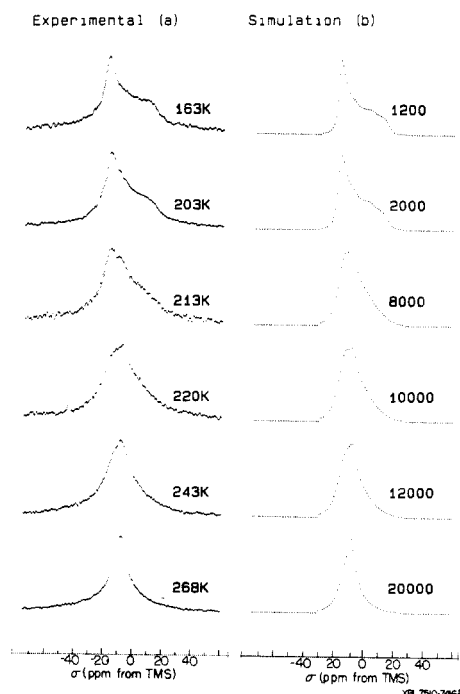


Figure 2. Experimental (a) and simulated (b) ^1H spectra of proton-doped (0.5%) hexagonal D_2O . Each simulation is labeled with the rate $\Omega = 1/\tau_c$.

parameters are reduced to zero by the rapid and isotropic reorientation in the liquid state. At intermediate temperatures, 240–267 K, the spectra show the characteristic features of slow molecular reorientation ($1/\tau_c \leq 200$ kHz). Spectrum integrals, I , are normalized by the spectrum integral obtained at 220 K and extrapolated to zero echo delay. At 240 K the spectral shape remains equivalent to the low-temperature static pattern, but there is substantial loss of signal intensity. The loss of signal intensity results from irreversible evolution due to molecular reorientation during the echo delay periods. As the temperature is raised and the dynamical rate approaches the quadrupolar coupling frequency, increased intensity loss is accompanied by narrowing of the pattern. At 267 K (some 9° below the freezing point) the pattern is nearly reduced to an isotropic line with intensity 1.5% of that observed in the low (rigid solid) limit.

The appearance of a narrow spectroscopic line (isotropically averaged coupling tensor) and exchange effects at temperatures below 220 K are also readily observed in the ^1H spectra of Figure 2a.¹⁰ These spectra were obtained from a sample of D_2O doped to 0.5% with protonated water. The spectral features arising from chemical shift anisotropy, seen at lower temperatures, are only resolved with the use of deuterium decoupling, the important details of which have been dealt with previously.^{10,14} The low-temperature slow-exchange-limit spectrum, obtained for $T \leq 200$ K, clearly shows the previously reported shielding anisotropy for water protons¹⁴ with $\sigma_{\parallel} = 15 \pm 2$ ppm and $\sigma_{\perp} = -19 \pm 2$ ppm (relative to TMS). Line-shape effects in the temperature range 210–240 K indicating reorientational rates exceeding the shielding anisotropy of 6 kHz are indeed apparent. The feature at the isotropic shift indicates reorientation by tetrahedral jumps rather than continuous rotational diffusion.^{10,15} Since these spectra are obtained with single-pulse excitation, the intensity losses discussed above for the ^2H experiment are absent.

When a picture for the reorientational dynamics in ice is proposed, the primary qualitative feature from our results is the appearance below the freezing point ($T_m - T \sim 10^\circ\text{C}$) of spectra with vanishing (^1H) or nearly vanishing (^2H) powder pattern anisotropy. Solid-state dynamics of limited amplitude, such as

(13) Jackson, J. A.; Rabideau, S. W. *J. Chem. Phys.* **1964**, *41*, 4008.

(14) Pines, A.; Ruben, D. J.; Vega, S.; Mehring, M. *Phys. Rev. Lett.* **1976**, *36*, 110.

(15) Spiess, H. W.; Sillescu, H. *J. Magn. Reson.* **1981**, *42*, 381.

(12) Waldstein, P.; Rabideau, S. W.; Jackson, J. A. *J. Chem. Phys.* **1964**, *41*, 3407.

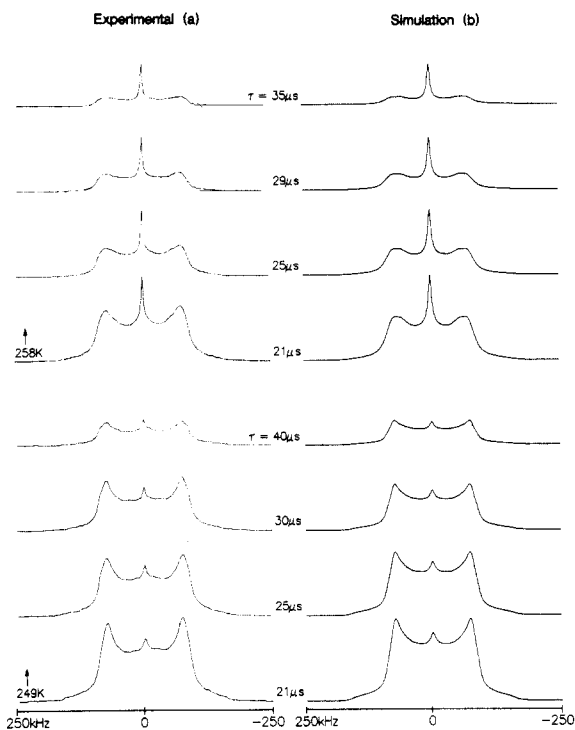


Figure 3. Experimental (a) and simulated (b) spectra for several echo delays, τ , at 249 and 258 K. The simulations used the rates $1/\tau_c = 2.5 \times 10^4 \text{ s}^{-1}$ at 258 K and $1/\tau_c = 1.2 \times 10^4 \text{ s}^{-1}$ at 249 K.

observed for methyl group rotation or water of hydration flipping so as to only interchange its deuterons, give rise to exchange-averaged patterns both larger in breadth and, in the case of the ^2H spectra, greater intensity than those observed here. Given these observations and the lattice symmetry for ice, a natural picture for water dynamics is jumping on the tetrahedral lattice with all four tetrahedral orientations equiprobable. Because of the high symmetry of this model, we need only specify the orientations of the unique coupling or shielding tensor axis. When this model is used,^{10,15,16} the experimental spectra (Figures 1a and 2a) were simulated by adjusting the single parameter τ_c , where $3\tau_c$ is the site lifetime. Line-shape simulations such as these work over the temperature range where relaxation is clearly dominated by reorientation; i.e., other contributions to the line width such as from residual dipolar couplings can reasonably be neglected. Thus, rates can be estimated in the range 240–267 K from the ^2H spectra and in the range 213–243 K from the ^1H spectra. The simulations in Figures 1b and 2b reproduce most of the features in the corresponding experimental spectra and are best described as nearly quantitative. Where the ^1H and ^2H results overlap at ~ 240 K, the rate is the same, and, as seen in Figure 1b, at each temperature the rate giving the optimal line-shape fit also gives a quantitative estimate of the ^2H NMR spectrum intensity. Substantial intensity losses have been predicted for tetrahedral jumps¹⁵ but not previously observed experimentally.

The model can be further tested at fixed temperatures by varying the solid-echo delay period in the ^2H NMR experiment during which the irreversible reorientational process is allowed to evolve. When the spectrum retains the appearance of the static limit, cf. those obtained at $T \leq 250$ K, the spectrum intensity is expected to decrease exponentially with time constant $\tau_c/2$ as the delay is increased (see ref 16, eq. 3.23e applied to the case of equiprobable tetrahedral jumps). Indeed, this is observed experimentally, and a rate of $1/\tau_c = 4.6 \times 10^3$ (240 K) is determined directly from the decay constant. Again, this temperature approaches the limit where other relaxation processes cannot be neglected, and thus the rate represents an upper limit. At higher

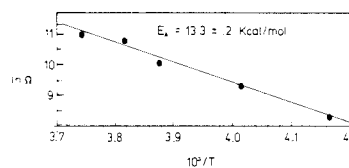


Figure 4. Activation energy for the jump rates, $1/\tau_c$, obtained from the ^2H spectra of Figure 1b.

temperatures, the relaxation is nonexponential, and direct line-shape simulation is required. Shown in Figure 3 are experimental spectra at two temperatures (249 and 258 K) and several different delay times. The corresponding simulations use the rate constants from Figure 1b and are in quantitative accord with experiment.

In the earlier single-crystal ^2H studies,¹² it was felt that the results indicated the absence of either isotropic molecular motion or hindered rotation about the O–D bonds even at temperatures as high as 263 K.¹² These studies employed continuous-wave techniques, equivalent to making the echo delay zero in the current study. Although it is experimentally unfeasible to obtain spectra with zero delay, the simulations of Figure 2b can be readily calculated for zero delay. Notice, as seen in Figures 1 and 3, the primary means for identifying reorientation at temperatures of 250 K or lower in the ^2H spectra is not by change in the pattern shape (contrary to the ^1H spectra) but rather loss of signal intensity. Thus, line shapes calculated with the τ_c of Figure 2b in the limit of zero echo delay are largely indistinguishable for $T \leq 250$ K. In effect, the use of the echo experiment allows one to study exchange processes at lower rates than is otherwise possible. Furthermore, the single-crystal work was carried out with a limited set of crystal orientations, the hexagonal axis either parallel or perpendicular to the magnetic field. The parallel orientation, for example, is particularly insensitive to slow exchange. Three of the sites have the unique tensor axis at the same angle relative to H_0 , 70.5° , and thus equivalent quadrupolar frequencies of ≈ 54 kHz. The fourth site is along H_0 , and the frequencies are ± 162 kHz. Consequently the only relevant jumps are those between orientations with the frequency difference of 216 kHz, which is large. Simulations show that frequency shifts occur only if the rate exceeds $5 \times 10^4 \text{ s}^{-1}$ or, based on Figure 1, $T > 260$ K. This may explain why the previous report¹³ of the quadrupolar coupling constant determined from a polycrystalline sample (all orientations observed) is substantially smaller. Temperature-dependent dynamics were indirectly alluded to in the previous work.^{12,13} Although spectra were readily obtained at the higher temperatures, no spectra were obtained for $T < 143$ K due to severe saturation (very long T_1). In our work we have roughly estimated the deuterium T_1 . It varies substantially with temperature from about 3–10 s at 265 K to over 100 s at 220 K. When the reorientational picture proposed here is used, these observed T_1 values are readily calculated with the τ_c of Figure 1b. Finally in this regard, we anticipate that some of the discrepancy may arise from differences in the samples. The samples used in this work are characteristic of commercial, spectroscopic grade solvent.

The rather substantial temperature dependence of the NMR spectra are in part due to the nonlinear manner in which the spectrum changes with τ_c as well as the substantial activation energy characterizing this dynamical process. The standard graph, Figure 4, shows a single activation energy, $E_A = 13.3 \pm 0.2$ kcal/mol, over the range 240–267 K. This value is, within error, equivalent to the $E_A = 13.5$ kcal/mol characterizing the Debye correlation time determined from dielectric relaxation for either protonated or deuterated water. Rates determined at lower temperature from the ^1H data indicate a lower activation energy. This is possibly due to a higher concentration of impurities in the sample.

In summary, these results show that, in a typical laboratory-quality sample of hexagonal ice, the constituent molecules are rotationally mobile. At 260 K, for example, each and every proton (deuteron) in a time of $\sim 100 \mu\text{s}$ explores the four tetrahedral orientations surrounding its bonded oxygen. The simple picture

(16) Wittebort, R. J.; Olejniczak, E. T.; Griffin, R. G. *J. Chem. Phys.* **1987**, *86*, 5411.

proposed here for reorientation by jumps on a tetrahedral lattice is certainly a simplification but is acceptable in this experimental context because the activation energy is large; i.e., the time in transit is negligible in comparison to the residence time. Both the activation energy and dynamical rates determined here are

directly comparable to those from dielectric relaxation.

Acknowledgment. Parts of this work were supported by the National Science Foundation (Grant DMB 8606358 to R.J.W.).

Registry No. Ice, 7732-18-5.

Quantum Chemical Studies of the Products of Decomposition of Anticancer (2-Haloethyl)nitrosoureas under Physiological Conditions

Anne-Marie Sapse,^{*,†‡} Evelyn B. Allen,[†] and J. William Lown^{*,§}

Contribution from The City University of New York, New York, New York 10031, John Jay College and Graduate Center, New York, New York 10019, Rockefeller University, New York, New York 10021, and Department of Chemistry, University of Alberta, Edmonton, Alberta, Canada T6G 2G2. Received June 24, 1987

Abstract: Ab initio (Hartree-Fock) calculations are performed on plausible intermediates leading to the observed products of decomposition of HENU's ((2-haloethyl)nitrosoureas) under physiological conditions. The entities investigated are diazohydroxides, diazonium ions, and diazoate salts. It is found that ethane- and 2-fluoroethanediazohydroxides are more prone to a soft electrophilic attack on the DNA bases than methane and 2-chloroethanediazohydroxides, and the same trend is found for their diazonium ions.

(2-Haloethyl)nitrosoureas (HENU's) have an established place in the clinical treatment of human malignancies, including Burkitt's lymphoma, Hodgkin's disease, and cerebral neoplasms.¹⁻³ It has been established that HENU's decompose spontaneously under physiological conditions, producing electrophiles, which attack sensitive cellular macromolecules, including DNA. Specific lesions have been identified, including base alkylation, cyclic nucleotide adduct formation, and interstrand cross-linking, the latter being a lethal event to the cell.^{5,6}

Simple nitrosoureas, such as methylnitrosourea, are highly mutagenic and carcinogenic, but more complex analogues, such as HENU's, have much higher antitumor activity in relation to their mutagenicity.⁷ It was found that the extent of the interstrand cross-linking correlates with activity against L-1210 murine leukemia and with the G + C content of the DNA.^{8,9} The sequence of reactions leading to interstrand cross-link formation by HENU's begins with the generation of reactive intermediates responsible for the transfer of the 2-haloethyl group to nucleophilic sites on the DNA bases. The monoadduct thus formed can then react with a nucleophilic site on another base, eliminate the halogen, and generate a cross-link consisting of an ethylene bridge. It has been shown that nucleophilic sites alkylated by 2-haloethyl groups comprise the O⁶ site on guanine as well as the N⁷ site, while the interstrand cross-linking sites that have been identified to date involve a cytosine amine group.^{6,10,11} The O⁶-alkylation leads to interstrand cross-linking, while the alkylation at N⁷ apparently does not lead directly to a cytotoxic event.

The ability to repair the alkylation at O⁶, before interstrand cross-linking can occur, has been related to the selective toxic action of HENU's. The tumor cell lines were found to be deficient in the removal of O⁶-methylguanine from their DNA and thus were found to belong to the phenotype termed Mer⁻, while normal cells belong to the phenotype Mer⁺, that is, show proficiency in removing O⁶-methylguanine from DNA.¹²

Therefore, the determination of the site of attack by the products of decomposition of HENU's under physiological conditions, as

well as their ability to form interstrand cross-links, becomes a crucial issue in respect to their antitumor activity and preferential cytotoxicity.

In order to establish the preferred site of attack, one also has to gather information about the nature of the intermediates in the decomposition, which result in the alkylating reactions. The possibility that a carbonium ion acts as the alkylating entity has been rejected.¹³ The putative alkylating agents are now considered to be either the 2-haloethanediazohydroxides or the corresponding kinetically equivalent diazonium ions.^{14,15} Kinetic experiments cannot distinguish between the latter species, and, therefore, it is of interest to study both species and to clarify their similarities

- (1) Ludlum, D. B. In *Mechanism of Action of 2-Haloethylnitrosoureas*; Becker F. F., Ed.; Plenum: New York, 1975; Vol. 5, p 285 ff.
- (2) Wheeler, G. P. *A Review of Studies on the Mechanism of Action of Nitrosoureas*; ACS Symposium Series 30; American Chemical Society: Washington, DC; p 87.
- (3) "Proceedings of the 7th New Drug Symposium on Nitrosoureas". *Cancer Treat. Rep.* **1976**, *60*, 651.
- (4) Singer, B.; Kusmierek, J. T. *Annu. Rev. Biochem.* **1982**, *51*, 655.
- (5) Lown, J. W.; McLaughlin, L. W.; Chang, Y. M. *Bioorg. Chem.* **1978**, *7*, 47.
- (6) Kohn, K. M. *Cancer Res.* **1977**, *37*, 1450.
- (7) Montgomery, J. A.; Johnston, T. P.; Shealy, Y. F. In *Medicinal Chemistry*, 4th ed.; Burger, A., Ed.; Wiley: New York.
- (8) Ludlum, D. H.; Kramer, B. S.; Wang, J.; Fenselau, C. *Biochemistry* **1975**, *14*, 5480.
- (9) Lown, J. W.; Gunn, B. C.; Chang, R. Y.; Majumdar, L. J. S. *Can. J. Biochem.* **1958**, *56*, 1006.
- (10) Stacey, K. A.; Cobb, M.; Cousens, S. F.; Alexander, P. *Ann. N.Y. Acad. Sci.* **1958**, *68*, 682.
- (11) Lawley, P. D.; Orr, D. J.; Jarman, M. *Biochem. J.* **1975**, *145*, 73.
- (12) Kohn, K. W.; Erickson, L. C.; Laurent, G.; Ducore, J.; Sharkey, N.; Ewig, K. A. *Nitrosoureas Current Status and New Developments*; Academic: New York, 1981; Chapter 6, pp 69-82.
- (13) Colvin, M.; Brundrett, R. *Nitrosoureas Current Status and New Developments*; Academic: New York, 1981; Chapter 4.
- (14) Lown, J. W. In *Synthesis and Properties of New Antileukemic 2-Haloethylnitrosoureas Based on an Analysis of the Reactions with DNA*; Bardos, T. J., Kalman, I. I., Eds.; Elsevier: New York, 1982; p 61.
- (15) (a) Lown, J. W.; Koganty, R. R.; Bhat, U. G.; Sapse, A. M.; Allen, E. B. *Int. J. Drugs Exptl. Clin. Invest.* **1986**, *XII*, 463. (b) Lown, J. W.; Chauhan, S. M. S.; Koganty, R. R.; Sapse, A. M. *J. Am. Chem. Soc.* **1984**, *106*, 6401.
- (16) Pearson, R. G. *Science (Washington, D.C.)* **1966**, *151*, 172.

[†]The City University of New York.

[‡]Rockefeller University.

[§]University of Alberta.